

Quadrupole collective models from the Hartree-Fock standpoint

Jacek Dobaczewski*

Service de Physique Théorique, Centre d'Etudes Nucléaires de Saclay, 91191 Gif-sur-Yvette CEDEX, France

Janusz Skalski

Soltan Institute for Nuclear Studies, PL-00-681 Warsaw, Poland

(Received 9 February 1989)

The assumptions underlying several quadrupole collective models are tested by a comparison with results of self-consistent Hartree-Fock plus BCS calculations using the Skyrme SIII interaction. We analyze the deformed states of ^{128}Ba in terms of condensates of fermion pairs which have been introduced in the interacting boson model and in the quadrupole phonon model, and in terms of multipole components of the density suggested by the Bohr and Mottelson model. We compare the deformation energy curves obtained by using (i) several multipole truncations of the Hartree-Fock plus BCS pairs, (ii) pairs obtained by a variation after truncation, and (iii) truncated series of multipole correlation energies. The influence of the core and vacuum polarization effects on the structure of the fermion pairs is found to be fairly strong.

I. INTRODUCTION

Over the past decades a considerable effort has been devoted to a description of a variety of properties of low-energy nuclear excitations in terms of relatively simple quadrupole collective models. The most studied (and used) among such models are the unified Bohr and Mottelson (BM) model,¹⁻³ and the interacting boson model (IBM) of Arima and Iachello.⁴ As far as the phase space of collective excitations is concerned, these models, together with the quadrupole phonon model (QPM) of Janssen, Jolos, and Dönau,⁵ are intimately related one to another.

The BM model assumes that the quadrupole collective states can be described by functions of quadrupole collective variables α_μ , $\mu = -2, \dots, +2$. The QPM, which makes a similar assumption for the many-boson states built out of the five components of the quadrupole boson operator b_μ^\dagger , has an identical phase space [due to the natural correspondence $b_\mu^\dagger = (\alpha_\mu - \partial/\partial\alpha_\mu^*)/\sqrt{2}$]. From the viewpoint of group theory, this phase space can be identified with an infinite sequence of the SU(5) representations, $N = 0, 1, \dots, \infty$, where N is the number of the b_μ^\dagger bosons. In the IBM, the collective states are built by means of the monopole and the quadrupole bosons, s^\dagger and d_μ^\dagger , and the total number N_0 of bosons is fixed. The IBM phase space can be associated with one representation of SU(6), and is identical to a finite sequence of the SU(5) representations for $N = 0, 1, \dots, N_0$, i.e., the IBM phase space is contained in that of the other two models.

This close geometrical relationship can be contrasted with the rather different microscopic interpretations proposed for these three models. The BM model assumes that the collective variable α_μ defines the shape of a nucleus, and refers to quadrupole distortions of the nuclear density. On the other hand, in the IBM and the QPM, the boson operators are associated with pairs of fermions

coupled to a given angular momentum J . In the QPM one considers pairs of *quasiparticles* coupled to $J = 2$ (\mathcal{D} pairs), while in the IBM the discussion is much in terms of pairs of valence *particles* (or holes past midshell) coupled to $J = 0$ and $J = 2$ (S and D pairs).

A possible test of the validity of the microscopic assumptions of the IBM and QPM consists of diagonalizing an effective fermion Hamiltonian in a space built with the fermion pairs appropriate for each model, and comparing the results with experimental data. However, such an ambitious program has, up to now, never been worked out. A simpler and tractable method, which we use in the present paper, consists of calculating the mean energy of an uncorrelated state built with the fermion pairs. This is feasible, because the lack of correlations allows one to use the Wick theorem to determine the energy of a fermion system with two-body interactions. This method provides only some weighted sums of collective energies instead of a complete collective spectrum to be compared with the experiment. However, from a comparison of these weighted sums with the energy resulting from the deformed mean-field theory, one can estimate the role of the angular momentum restrictions on the structure of the fermion pairs suggested by the IBM and the QPM.

There have already been several attempts to derive the microscopic foundations of the IBM from the deformed mean-field theory⁶⁻¹⁸ (see also the review by Iachello and Talmi¹⁹). In the present paper, which follows our rapid communication,²⁰ we analyze the assumptions of the IBM, QPM, and the BM model from the point of view of the deformed self-consistent Hartree-Fock (HF) approach.

Our study differs from the previous ones⁶⁻¹⁸ by one or more of the following elements. (i) We investigate fermion pairs defined with respect to several reference vacuums. Up to now, the only considered vacuum was the closed-shell inert core suggested by the IBM. As in Ref.

20, we also consider the vacuum suggested by the QPM, i.e., the spherical state of the studied nucleus. This allows for a consistent comparison of the microscopic foundations of the IBM and QPM. (ii) Previous calculations have been performed within a rather restricted single-particle space. Since we free ourselves from this restriction, we can study the influence of polarization effects. (iii) We use the Hartree-Fock theory with a realistic effective interaction (Skyrme SIII), instead of the separable residual quadrupole-quadrupole force, which has mainly been used up to now. Therefore, our HF energy directly compares with the nuclear mass, and the deformation energy and equilibrium deformation are properly determined. (iv) We not only calculate the properties of states made of the low-angular-momentum components of the HF pairs (truncation after variation), but we also perform a full minimization for fixed multipole contents of the fermion pairs (variation after truncation). We can therefore determine the absolute lower bounds for the energy of the deformed states in the frame of the IBM and QPM. (v) In order to compare the effects of truncations inherent to the IBM and QPM with those of the BM model, we calculate the multipole correlation energies corresponding to the low angular-momentum components of the density matrix and estimate the effect of neglecting all but the quadrupole correlations.

The paper is organized as follows. In Sec. II we present the results of the HF method for the deformed states of ^{128}Ba . In Sec. III we give details of our method to analyze the assumptions made in the IBM and QPM. In particular, we discuss the relationship between the two associated vacuums and their two coherent fermion pairs. In Sec. IV we present the results obtained for truncated HF pairs, while Sec. V contains those obtained by a variation after truncation. Section VI describes the calculation of the correlation energies, and our conclusions are given in Sec. VII.

II. DEFORMED STATES OF ^{128}Ba

Our choice of the nucleus ^{128}Ba for testing the microscopic foundations of the interacting boson model (IBM) and of the quadrupole phonon model (QPM) is motivated by two observations: (i) this nucleus has a relatively small calculated ground-state hexadecapole moment, which simplifies the discussion of the quadrupole effects, and (ii) the prolate and oblate minima are almost equally deep,²¹ which allows us to discuss the effects occurring for both shapes. In the present paper the deformed states of ^{128}Ba are calculated within the constrained Hartree-Fock (CHF) theory^{22,23} with the Skyrme SIII interaction²⁴ and the pairing correlations are included by the BCS method. The axial, parity, and time-reversal symmetries are imposed when solving the HF equations. The dependence of the HF states on deformation is obtained by using the quadrupole moment $\hat{Q} = \sum_{i=1}^A (2z_i^2 - x_i^2 - y_i^2)$ as the constraining operator. The HF solutions are found by expanding the single-particle wave functions on the spherical harmonic oscillator basis including states with the principal quantum number $N_0 \leq 12$. The value of the oscillator basis parameter²³ $b = \sqrt{m\omega/\hbar} = 0.48 \text{ fm}^{-1}$ is

determined by minimizing the HF energy at the spherical shape.

Two elements of our approach should be stressed. Firstly, we use the self-consistent method with a realistic two-body interaction, which provides us with a variational estimate of the total energy of the nuclear system. A quality of any approximation concerning the structure of the nuclear wave function can therefore be immediately judged by looking at the corresponding increase of the variational energy. Secondly, we explicitly use a large basis of the single-particle states and neither restrict the calculation to a valence space nor assume any inert core. This allows us to study the effects of the core polarization and of the vacuum polarization (i.e., the role of the single-particle states below and above the valence space, respectively), and also to disregard the problem of effective charges, inherent to calculations which use a restricted space.

Two different treatments of pairing correlations have been used in the present study. In the first one, we have used the constant²² (independent of the deformation) gap parameters,

$$\Delta_n = 1.41 \text{ MeV}, \quad \Delta_p = 1.38 \text{ MeV}, \quad (2.1)$$

for neutrons and protons, respectively, which have been determined from the experimental odd-even mass differences.²⁵ The $\Delta = \text{const}$ approach is, as discussed in Ref. 22, equivalent to a minimization of the quantity

$$E' = E_F + 2E_P, \quad (2.2)$$

where E_F is the mean-field energy equal to the expectation value of the kinetic energy operator plus the expectation value of the Skyrme interaction, while the pairing energy E_P is given in terms of the standard BCS coefficients u_μ and v_μ by

$$E_P = -\Delta_n \sum_{\mu > 0, n} u_\mu v_\mu - \Delta_p \sum_{\mu > 0, p} u_\mu v_\mu. \quad (2.3)$$

The summation over $\mu > 0, n(p)$ denotes the summation over the single-particle neutron (proton) states which have positive projections Ω of the angular momentum on the quantization axis.

In the second version of the BCS method, which we call the $G = \text{const}$ approach, one solves the BCS equations for a monopole pairing interaction with fixed (independent of the deformation) strengths G_n and G_p for neutrons and protons, respectively. Such approach is equivalent to minimizing the total energy

$$E = E_F + E_P, \quad (2.4)$$

where the pairing energy is given by

$$E_P = -G_n \left[\sum_{\mu > 0, n} u_\mu v_\mu \right]^2 - G_p \left[\sum_{\mu > 0, p} u_\mu v_\mu \right]^2. \quad (2.5)$$

The *unrestricted* variation of both functionals, Eqs. (2.2) and (2.4), yields exactly the same solution if the pairing gaps are related to the pairing strengths by

$$\begin{aligned}\Delta_n &= G_n \sum_{\mu>0,n} u_\mu v_\mu, \\ \Delta_p &= G_p \sum_{\mu>0,p} u_\mu v_\mu.\end{aligned}\quad (2.6)$$

Because of the deformation-dependent density of the single-particle levels, relations (2.6) can in general be fulfilled only for a single value of deformation. In the present study we have adopted for the $G = \text{const}$ approach the values

$$G_n = 0.0955 \text{ MeV}, \quad G_p = 0.1091 \text{ MeV}, \quad (2.7)$$

which at the deformation $Q = 8b$, close to the equilibrium deformation of ^{128}Ba , fulfill relations (2.6) with the pairing gaps of Eq. (2.1).

Some care should be taken when interpreting the results of the $\Delta = \text{const}$ calculations, because the quantity minimized, Eq. (2.2), is not then equal to the energy, Eq. (2.4). In particular, one can encounter the situation (see the results of variation after truncation, Sec. V) when the energy *increases* for enlarged variational space. In such a case, a quality of the restricted variational wave function can be judged by comparing the corresponding values of E' , Eq. (2.2).

In Fig. 1 we present the pairing energy E_p obtained for ^{128}Ba in our two versions of the BCS approach. For $\Delta = \text{const}$, the pairing energy depends weakly on deformation, and has a shallow minimum at the spherical point, which is related to an increase of the level density close to the Fermi surface. The fluctuations of the pairing energy are strongly amplified for $G = \text{const}$, and the minimum at the spherical shape becomes very deep. The amplification is strong because all single-particle levels (with $N_0 \leq 12$) have been purposely used when solving the BCS equations. The best physical description of pairing correlations can probably be found somewhere in between our $\Delta = \text{const}$ and $G = \text{const}$ results. In the present study, however, we prefer to keep both extremes, which allows us to discuss the influence of pairing effects on our conclusions concerning the microscopic foundations of

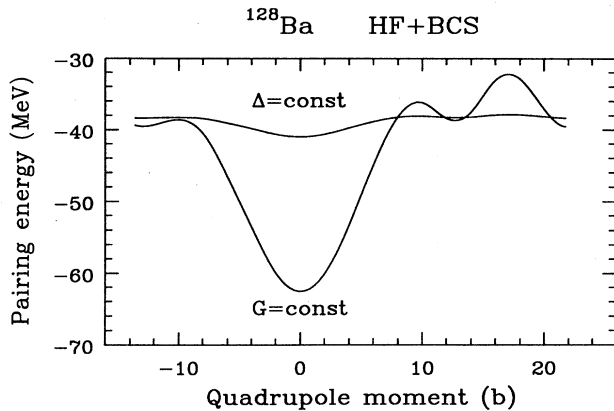


FIG. 1. Pairing energy of ^{128}Ba obtained by the $\Delta = \text{const}$ and the $G = \text{const}$ versions of the BCS approach.

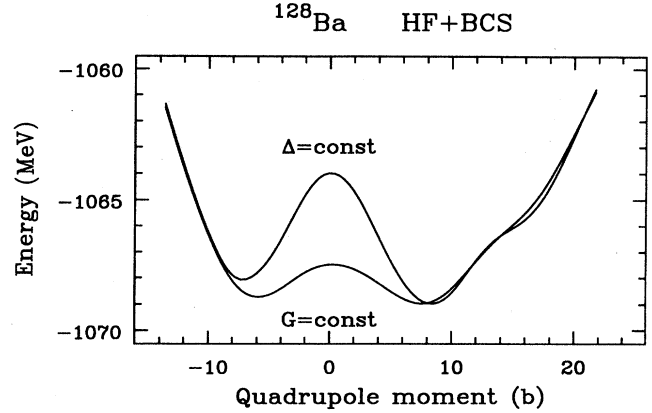


FIG. 2. Hartree-Fock energy of ^{128}Ba obtained for pairing correlations described by the $\Delta = \text{const}$ and the $G = \text{const}$ versions of the BCS approach.

the IBM and QPM.

In Fig. 2 we plot the total energy E as function of deformation. The strong decrease of the pairing energy at the spherical shape for $G = \text{const}$ results in a decrease of the total energy at this shape. The prolate deformation energy is decreased in this way from 5 to 1.5 MeV. Beyond the prolate and oblate minima the influence of pairing correlations on the total energy is small.

III. REFERENCE STATES AND PAIR CONDENSATES

The deformed nuclear state $|\Psi\rangle$ resulting from the HF method is a quasiparticle vacuum for the set of the quasiparticle annihilation operators, which we denote by β_μ , i.e., $\beta_\mu|\Psi\rangle = 0$. The quasiparticle creation and annihilation operators, β_μ^\dagger and β_μ , are related to the particle creation and annihilation operators, a_μ^\dagger and a_μ , by the Bogolyubov transformation

$$\begin{pmatrix} \beta^\dagger \\ \beta \end{pmatrix} = \begin{pmatrix} A^T & B^T \\ B^\dagger & A^\dagger \end{pmatrix} \begin{pmatrix} a^\dagger \\ a \end{pmatrix}. \quad (3.1)$$

In view of the Thouless theorem the quasiparticle vacuum $|\Psi\rangle$ can be expressed in terms of the bare vacuum $|0\rangle, a_\mu|0\rangle = 0$, as

$$|\Psi\rangle = \langle 0|\Psi\rangle \exp\{\hat{C}^\dagger\}|0\rangle, \quad (3.2)$$

where \hat{C}^\dagger is the coherent particle pair creation operator

$$\hat{C}^\dagger = \frac{1}{2} \sum_{\mu\nu} C_{\mu\nu}^\dagger a_\mu^\dagger a_\nu^\dagger. \quad (3.3)$$

The antisymmetric matrix $C_{\mu\nu}$ is related to the coefficients of the Bogolyubov transformation, Eq. (3.1), by

$$C = -BA^{-1}. \quad (3.4)$$

Because $|\Psi\rangle$ has the form of a sum of powers of \hat{C}^\dagger acting on vacuum, Eq. (3.2), one can call it the condensate of the particle pairs \hat{C}^\dagger .

The diagram in Fig. 3 presents various Bogolyubov

transformations which will be discussed in this section. Transformation (3.1) is represented by the vertical arrow connecting the box $a_\mu|0\rangle$ with the box $\beta_\mu|\Psi\rangle$, while the corresponding Bogolyubov matrices A and B , together with the pair matrix C , are marked within the oval box at the middle of the arrow. Let the state $|\Psi_{\text{ref}}\rangle$, which we call the reference state, be an arbitrary quasiparticle state. Denoting the quasiparticle operators related to $|\Psi_{\text{ref}}\rangle$ by α_μ^\dagger and α_μ , i.e., $\alpha_\mu|\Psi_{\text{ref}}\rangle=0$, we can express β_μ^\dagger and β_μ in terms of α_μ^\dagger and α_μ by the following Bogolyubov transformation (see Fig. 3):

$$\begin{pmatrix} \beta^\dagger \\ \beta \end{pmatrix} = \begin{pmatrix} U^T & V^T \\ V^\dagger & U^\dagger \end{pmatrix} \begin{pmatrix} \alpha^\dagger \\ \alpha \end{pmatrix}, \quad (3.5)$$

which allows us to present $|\Psi\rangle$ in terms of the reference state $|\Psi_{\text{ref}}\rangle$ as

$$|\Psi\rangle = \langle \Psi_{\text{ref}} | \Psi \rangle \exp\{\hat{Z}^\dagger\} |\Psi_{\text{ref}}\rangle, \quad (3.6)$$

where the coherent quasiparticle pair creation operator \hat{Z}^\dagger is given by

$$\hat{Z}^\dagger = \frac{1}{2} \sum_{\mu\nu} Z_{\mu\nu}^\dagger \alpha_\mu^\dagger \alpha_\nu^\dagger, \quad (3.7)$$

and

$$Z = -VU^{-1}. \quad (3.8)$$

Therefore, the deformed state $|\Psi\rangle$, being the condensate of the particle pairs \hat{C}^\dagger , Eq. (3.2), can also be considered as a condensate of the coherent quasiparticle pairs \hat{Z}^\dagger , built on an *arbitrary* reference state $|\Psi_{\text{ref}}\rangle$, of the corresponding quasiparticle creation operators α_μ^\dagger .

For a given deformed state $|\Psi\rangle$ one can easily find the relation between the particle pair \hat{C}^\dagger and the quasiparticle pair \hat{Z}^\dagger . To this end, let us suppose that the reference state is determined by the Bogolyubov transformation relating α_μ^\dagger and α_μ and the particle operators a_μ^\dagger and a_μ (Fig. 3),

$$\begin{pmatrix} \alpha^\dagger \\ \alpha \end{pmatrix} = \begin{pmatrix} A_{\text{ref}}^T & B_{\text{ref}}^T \\ B_{\text{ref}}^\dagger & A_{\text{ref}}^\dagger \end{pmatrix} \begin{pmatrix} a^\dagger \\ a \end{pmatrix}, \quad (3.9)$$

i.e.,

$$|\Psi_{\text{ref}}\rangle = \langle 0 | \Psi_{\text{ref}} \rangle \exp\{\hat{C}_{\text{ref}}^\dagger\} |0\rangle, \quad (3.10)$$

$$\hat{C}_{\text{ref}}^\dagger = \frac{1}{2} \sum_{\mu\nu} (C_{\text{ref}}^\dagger)_{\mu\nu} a_\mu^\dagger a_\nu^\dagger, \quad (3.11)$$

$$C_{\text{ref}} = -B_{\text{ref}} A_{\text{ref}}^{-1}. \quad (3.12)$$

Expressing the Bogolyubov transformation (3.1) as the superposition of transformations (3.9) and (3.5), one obtains from (3.4) that

$$C = (A_{\text{ref}}^* Z - B_{\text{ref}}) (A_{\text{ref}} - B_{\text{ref}}^* Z)^{-1}, \quad (3.13)$$

which can be inverted, and gives

$$Z = (A_{\text{ref}}^T C - B_{\text{ref}}^T) (A_{\text{ref}}^\dagger - B_{\text{ref}}^\dagger C)^{-1}. \quad (3.14)$$

Since the rotational invariance is broken in a deformed state, the pair operator \hat{Z}^\dagger contains various angular momentum components:

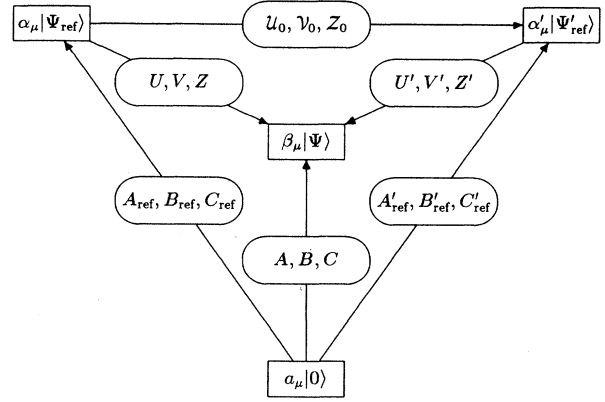


FIG. 3. A schematic illustration of the relationship between various Bogolyubov transformations discussed in the text. Each rectangular box represents a quasiparticle vacuum. Bogolyubov transformations are denoted by arrows connecting rectangular boxes. The oval boxes attached to the arrows embrace the matrices of the Bogolyubov transformation and the corresponding pair matrix.

$$\hat{Z}^\dagger = \sum_J x_J \hat{Z}_J^\dagger, \quad (3.15)$$

where $\hat{Z}_J^\dagger = \frac{1}{2} \sum_{\mu\nu} (Z_J^\dagger)_{\mu\nu} \alpha_\mu^\dagger \alpha_\nu^\dagger$ transforms under spatial rotations as the rank J spherical tensor, and the coefficients x_J are fixed by requiring that for each J one has

$$2 \langle \Psi_{\text{ref}} | \hat{Z}_J \hat{Z}_J^\dagger | \Psi_{\text{ref}} \rangle = \sum_{\mu\nu} |(Z_J)_{\mu\nu}|^2 = 1. \quad (3.16)$$

The sum in Eq. (3.15) contains in general all values of J , and also, for each J , all values of the magnetic quantum number M (which is not shown explicitly). For the deformed states $|\Psi\rangle$ which conserve some spatial symmetries, the sum can be restricted to some particular values of J and M . In the present study we consider axial and parity invariant deformed states, in which case only the even- J and $M=0$ components appear in Eq. (3.15).

From Eq. (3.14) it is clear that the multipole composition of the quasiparticle pair \hat{Z}^\dagger depends, for a given $|\Psi\rangle$ i.e., for a fixed matrix C , on the choice of the reference state. When the reference state $|\Psi_{\text{ref}}\rangle$ conserves the rotational symmetry, which we will assume from now on, the matrices A_{ref} and B_{ref} defining the Bogolyubov transformation (3.9) transform as scalars. Even then the multipole components of \hat{Z}^\dagger depend on the choice of the reference state, which is a consequence of the nonlinearity of the relation between the quasiparticle pair matrix Z and the nonscalar particle-pair matrix C , Eq. (3.14).

In order to get a closer insight into the dependence of \hat{Z}_J^\dagger on the reference state, let us suppose that we have two different reference states $|\Psi_{\text{ref}}\rangle$ and $|\Psi'_{\text{ref}}\rangle$. The quasiparticle operators related to $|\Psi'_{\text{ref}}\rangle$ will be denoted by α'_μ^\dagger and α'_μ , i.e., $\alpha'_\mu|\Psi'_{\text{ref}}\rangle=0$, while the primed matrices U' , V' , Z' , A'_{ref} , B'_{ref} and C'_{ref} will refer to $|\Psi'_{\text{ref}}\rangle$ through equations analogous to those from Eq. (3.5) to Eq. (3.12). Let us also denote by U_0 , V_0 , and Z_0 the matrices determining the reference state $|\Psi'_{\text{ref}}\rangle$ in terms of the reference

state $|\Psi_{\text{ref}}\rangle$ (Fig. 3), i.e.,

$$\begin{pmatrix} \alpha'^{\dagger} \\ \alpha' \end{pmatrix} = \begin{pmatrix} \mathcal{U}_0^T & \mathcal{V}_0^T \\ \mathcal{V}_0^{\dagger} & \mathcal{U}_0^{\dagger} \end{pmatrix} \begin{pmatrix} \alpha^{\dagger} \\ \alpha \end{pmatrix}, \quad (3.17)$$

$$|\Psi'_{\text{ref}}\rangle = \langle \Psi_{\text{ref}} | \Psi'_{\text{ref}} \rangle \exp\{\hat{Z}_0^{\dagger}\} |\Psi_{\text{ref}}\rangle, \quad (3.18)$$

$$\hat{Z}_0^{\dagger} = \frac{1}{2} \sum_{\mu\nu} (Z_0^{\dagger})_{\mu\nu} \alpha_{\mu}^{\dagger} \alpha_{\nu}^{\dagger}, \quad (3.19)$$

$$Z_0 = -\mathcal{V}_0 \mathcal{U}_0^{-1}. \quad (3.20)$$

The relation between the quasiparticle matrices Z and Z' can now be derived, similarly to the derivation of Eqs. (3.13) and (3.14). Comparing the Bogolyubov transformation $|\Psi_{\text{ref}}\rangle \rightarrow |\Psi\rangle$, Eq. (3.5), with the superposition of two Bogolyubov transformations $|\Psi_{\text{ref}}\rangle \rightarrow |\Psi'_{\text{ref}}\rangle \rightarrow |\Psi\rangle$ (see Fig. 3) one obtains

$$Z' = \mathcal{U}_0^T (Z - Z_0) (I + Z_0^{\dagger} Z)^{-1} \mathcal{U}_0^{\dagger -1}. \quad (3.21)$$

As seen in Eq. (3.21), the relation between the quasiparticle pair matrices Z' and Z , corresponding to two reference states, $|\Psi'_{\text{ref}}\rangle$ and $|\Psi_{\text{ref}}\rangle$, is again nonlinear, and therefore there is no simple correspondence between the multipole components of these two matrices. Even a single multipole component of the Z matrix gives in general rise to all multipole components of the Z' matrix. However, the presence of the difference $Z - Z_0$ in Eq. (3.21) allows us to formulate an approximate conclusion concerning the scalar ($J=0$) component of Z' . Noticing that the matrices \mathcal{U}_0 , \mathcal{V}_0 , and Z_0 are scalars [this is so because the Bogolyubov transformation (3.17) connects two spherically symmetric reference states, $|\Psi_{\text{ref}}\rangle$ and $|\Psi'_{\text{ref}}\rangle$] it is clear that the scalar component of Z' is strongly reduced whenever the Z_0 matrix is close to the scalar component of the Z matrix.²⁶

Such a reduction of the scalar component is at the origin of the \mathcal{D} dominance²⁰ in the quadrupole phonon model⁵ (QPM), as opposed to the S - \mathcal{D} dominance^{9,10} in the interacting boson model.⁴ Following Ref. 20, we study here the assumptions of both models by considering a choice of the two corresponding reference states.

In the IBM, the collective states of a given nucleus are described in terms of pairs of valence particles (or holes past midshell) added to the nearest closed shell nucleus. Therefore, in order to analyze the deformed HF states of ^{128}Ba , Sec. II, in terms of the IBM, we choose the IBM reference state (IBM core) to be the spherical HF ground state of the ^{132}Sn nucleus. This reference state will be denoted by $|\Psi_{\text{ref}}\rangle$, and the corresponding Bogolyubov transformations and pair matrices will be denoted accordingly (see Fig. 3). In Fig. 4(a) we schematically illustrate the principal idea of the choice of the IBM core by presenting the quasiparticle states according to their particle number A and quadrupole moment Q . The bare vacuum $|0\rangle$, which has $A=0$ and $Q=0$, is placed at the origin of the figure. The IBM reference state $|\Psi_{\text{ref}}\rangle$ is placed at $Q=0$ and $A=132$, while the deformed state $|\Psi\rangle$ of ^{128}Ba is placed at $Q>0$ and $A=128$. The Bogolyubov transformation $|0\rangle \rightarrow |\Psi\rangle$, Eq. (3.1), increases both the particle number and the quadrupole moment. The transformation $|0\rangle \rightarrow |\Psi_{\text{ref}}\rangle$, Eq. (3.9), increases only

the particle number, while $|\Psi_{\text{ref}}\rangle \rightarrow |\Psi\rangle$, Eq. (3.5), increases the quadrupole moment and removes some particles. (In fact, it adds some protons and removes some neutrons, which is not essential in a schematic discussion.)

In the QPM, the collective states are assumed to be built of coherent two-quasiparticle excitations added to the spherical state of the given nucleus. Therefore we choose the OPM reference state (QPM core) (which will be denoted by $|\Psi'_{\text{ref}}\rangle$) to be the HF solution for ^{128}Ba obtained by imposing the spherical symmetry when solving the HF equations. In Fig. 4(b) we present, in analogy to Fig. 4(a), the idea underlying the choice of the QPM

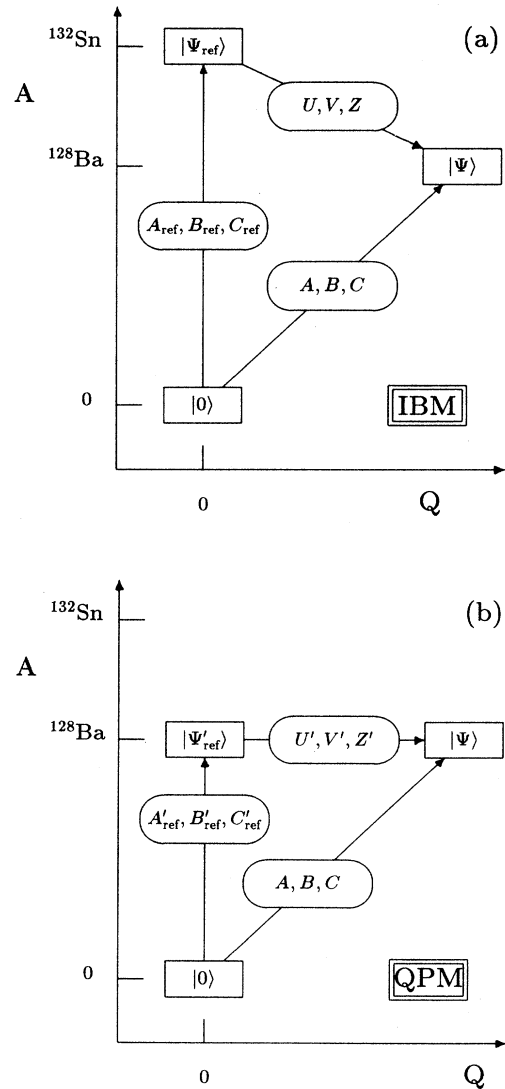


FIG. 4. A schematic illustration of the choice of the reference state in the IBM (a) and in the QPM (b). The rectangular boxes represent the quasiparticle vacuums, and are placed in the diagram according to their particle number A and quadrupole moment Q . The arrows and oval boxes denote Bogolyubov transformations.

reference state. Contrary to the IBM, the Bogolyubov transformation $|\Psi'_{\text{ref}}\rangle \rightarrow |\Psi\rangle$ does not change the particle number and only creates an appropriate quadrupole moment. Since the transformations $|\Psi_{\text{ref}}\rangle \rightarrow |\Psi\rangle$ and $|\Psi_{\text{ref}}\rangle \rightarrow |\Psi'_{\text{ref}}\rangle$, Eq. (3.17), change the neutron and proton numbers in the same way, the scalar pair matrix Z_0 is not far from the scalar component of the IBM pair matrix Z , and the cancellation in Eq. (3.21) leads to a depletion of the scalar part of the QPM pair matrix Z' . Denoting the multipole components Z_J of the IBM pair matrix by S, D, G, \dots for $J=0, 2, 4, \dots$, respectively, and the respective multipole components Z'_J of the QPM pair matrix $\mathcal{S}, \mathcal{D}, \mathcal{G}, \dots$, we can formulate the above result as the \mathcal{D} dominance in the QPM being a result of the S - \mathcal{D} dominance in the IBM.

Before discussing the influence of various truncations of the multipole components of the IBM and QPM pairs on the nuclear properties, Sec. IV, let us make two remarks concerning the IBM and QPM reference states. Firstly, we want to stress that both reference states have been calculated self-consistently by using the same HF method which has been used to determine the deformed states of ^{128}Ba , Sec. II, i.e., the same force parameters (SIII), numerical approximations and numerical code have been used. Since two versions of approach to the pairing correlations, $G = \text{const}$ and $\Delta = \text{const}$, see Sec. II, have been used when determining the deformed states, also two corresponding QPM reference states have been calculated. Secondly, one should note that the use of the BCS method for the closed shell nucleus ^{132}Sn results in the vanishing of the pairing correlations, and yields the ordinary HF solution. In such a case the IBM reference state $|\Psi_{\text{ref}}\rangle$ is exactly orthogonal to the bare vacuum $|0\rangle$ and the Thouless theorem, Eq. (3.10), is not applicable, because of the singularity of the A_{ref} matrix in Eq. (3.12). In order to avoid the use of a separate set of formulae, relevant in such a case, we have performed the determination of the ground state of ^{132}Sn with fixed and insignificantly small value of the pairing gap parameters, $\Delta_n = \Delta_p = 0.1$ MeV, and checked that none of the results depend on a change of this particular value.

IV. TRUNCATION OF THE HF PAIRS

In this section we discuss the results of calculations for truncated quasiparticle pairs \hat{Z}^\dagger and \hat{Z}'^\dagger , corresponding to the IBM and the QPM reference states $|\Psi_{\text{ref}}\rangle$ and $|\Psi'_{\text{ref}}\rangle$, respectively, which were described in Sec. III. The truncation consists in keeping only selected terms in the multipole expansion of the quasiparticle pairs, Eq. (3.15),

$$\hat{Z}^\dagger = \sum_{J=J_{\text{min}}}^{J_{\text{max}}} x_J \hat{Z}_J^\dagger. \quad (4.1)$$

The truncated pair \hat{Z}^\dagger is denoted by a tilde. The truncation of the quasiparticle pairs leads to truncated HF states given by

$$|\tilde{\Psi}\rangle = \langle \Psi_{\text{ref}} | \tilde{\Psi} \rangle \exp\{\hat{Z}^\dagger\} | \Psi_{\text{ref}} \rangle. \quad (4.2)$$

In order to determine the HF energy of this state, as well as mean values of other observables, one has to calculate the corresponding density matrix and the pairing tensor. An efficient way to do this consists in using Eq. (3.13) to calculate the particle pair matrix $C(\tilde{Z})$, corresponding to the truncated quasiparticle pair matrix \tilde{Z} , and then finding the canonical form of $C(\tilde{Z})$,

$$C(\tilde{Z})_{\mu\nu} = s_\mu^* c_\mu \delta_{\bar{\mu}\nu}, \quad (4.3)$$

which can be done by diagonalizing $C(\tilde{Z})^\dagger C(\tilde{Z})$. The index $\bar{\mu}$ refers to the time reversed single-particle state, and s_μ^* is the phase factor associated with the time-reversal, $\hat{T}|\mu\rangle = s_\mu^* |\bar{\mu}\rangle$. The BCS coefficients can now be determined as

$$u_\mu = \frac{1}{(1+c_\mu^2)^{1/2}}, \quad v_\mu = \frac{c_\mu}{(1+c_\mu^2)^{1/2}}, \quad (4.4)$$

which allows to calculate the density matrix $\rho_{\mu\nu} = v_\mu^2 \delta_{\mu\nu}$, and hence, the mean-field Hartree-Fock energy, as well as the pairing energy, Eq. (2.3) or (2.5). When the BCS coefficients u_μ and v_μ are determined from the BCS equations, the product $u_\mu v_\mu$ has the same sign for all μ . However, it is important to notice that this need not to be the case when they are determined from a pair matrix through Eqs. (4.3) and (4.4). Therefore, a partial cancellation is possible in the sums determining the pairing energy, Eq. (2.3) or (2.5).

As discussed in Sec. II, we have performed two versions of HF calculations, which differ by the treatment of the pairing correlations, and are referred to as the $\Delta = \text{const}$ and the $G = \text{const}$ version. The result for the $\Delta = \text{const}$ version has already been presented in Ref. 20, and therefore in this section we consider the $G = \text{const}$ version, unless we explicitly mention the other one.

The coefficients x_J , Eq. (3.15), give the relative amplitudes of various multipole components of the HF pairs. They have been presented in Fig. 1 of Ref. 20 for the $\Delta = \text{const}$ version. The results for $G = \text{const}$ are almost identical, and therefore are not reported here. In both versions of pairing treatment one obtains the dominance of the \hat{Z}_0^\dagger and \hat{Z}_2^\dagger pairs (S - \mathcal{D} dominance) for the IBM and of the $\hat{Z}_2^{\prime\dagger}$ pair (\mathcal{D} dominance) for the QPM.

From the S - \mathcal{D} and the \mathcal{D} dominance one cannot directly infer that the description of deformed states in terms of low angular-momentum components of fermion pairs is accurate enough. Since the deformed state Eq. (3.6) results from the exponentiation of the coherent pair Eq. (3.7), the dominant low- J components lose in importance while the nondominant ones gain, and this is so because of the cancellation due to the Pauli principle. The accuracy of such a description can only be discussed by calculating observables for the truncated states, Eq. (4.2), and comparing them with the untruncated HF values. For the IBM quasiparticle pairs we have performed the calculations for the truncation to the angular momenta 0, 02, 024, 0246, 02468, and 0...10. Although keeping the $J=0$ (S) component alone cannot give a correct description, because the $J=2$ (\mathcal{D}) component is equally large, it can give us some insight into the structure of the S pair. For the QPM we have used the truncations to 2, 24, 246,

02, 024, and 0246. In all cases the dominant $J=2$ component is included, while the first three truncations differ from the last three ones by an absence of the $J=0$ (\mathcal{S}) component. Again such choice allows us to discuss a role of the \mathcal{S} pair.

A. Multipole moments and particle numbers

In Figs. 5 and 6 we show the quadrupole and the hexadecapole moments, respectively, calculated for the truncated HF states, Eq. (4.2). The results are plotted as functions of the untruncated HF quadrupole moment. In Fig. 5(a) (IBM) it is seen that the major part of the HF quadrupole moment is reproduced by the dominant (02) components in the whole deformation range. After including the $J=4$ component, the truncated quadrupole moment becomes identical to the HF value within the precision of the figure. For the QPM core, Fig. 5(b), the major part is also given by the dominant (2) component. Inclusion of either $J=0$ or $J=4$ component gives almost the exact value, while inclusion of both of them reproduces the HF quadrupole moment exactly. The hexadecapole moment is for both cores reproduced nearly correctly after inclusion of $J=0, 2$, and 4 components. However, when only the dominant components are kept, its overall dependence on the deformation is also reproduced.

Before proceeding with the comparison of energies of the truncated states it is necessary to mention that the truncation affects the expectation value of the particle number. The HF state has the correct mean values of neutron and proton numbers, but these are changed after removal of some components of the HF pairs. This is shown in Figs. 7(a) and (c) for the IBM core and in Figs. 7(b) and (d) for the QPM core. For the IBM core, the proton numbers in truncated states are larger than the correct value of $Z=56$, while the neutron numbers are smaller than $N=72$. The difference in the studied range of deformations may be as large as 10 neutrons or 12 protons, when only the dominant components are kept. One reproduces the correct values with a sufficient precision only after including all components up to $J=8$. Let us note that these changes are opposite to what one might

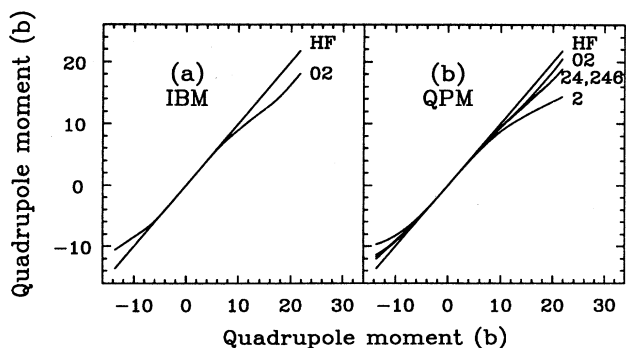


FIG. 5. Quadrupole moment of truncated states, for the IBM (a) and the QPM (b) reference state, compared with the HF results.

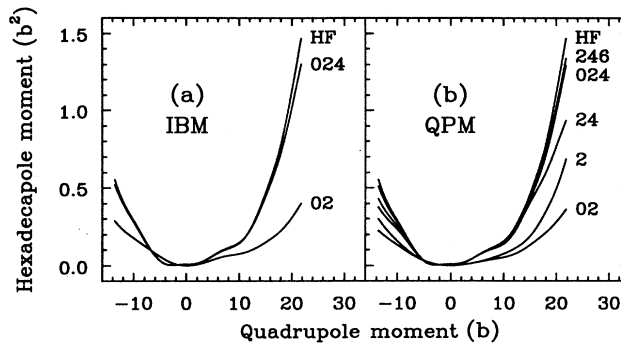


FIG. 6. Hexadecapole moment of truncated states, for the IBM (a) and the QPM (b) reference state, compared with the HF results.

expect from naive considerations. Indeed, had the proton (neutron) pairs been the pure valence particle-particle (hole-hole) pairs, the proton (neutron) number would have had to be smaller (larger) for truncated pairs than for the untruncated ones. The actual results are different, because the nondominant components have large amplitudes outside the valence space (see discussion later in section). For the QPM core, the particle numbers are much closer to the correct values, at least in a wide range of deformations extending beyond the prolate and oblate equilibrium deformations. For the far end of the prolate deformation, the discrepancy reaches, however, as much as seven neutrons and six protons.

B. Energies

The differences in particle numbers prevent a direct comparison of energies calculated for the truncated states, Eq. (4.2), with the corresponding HF energies. Since the binding energy per particle is around 8 MeV,

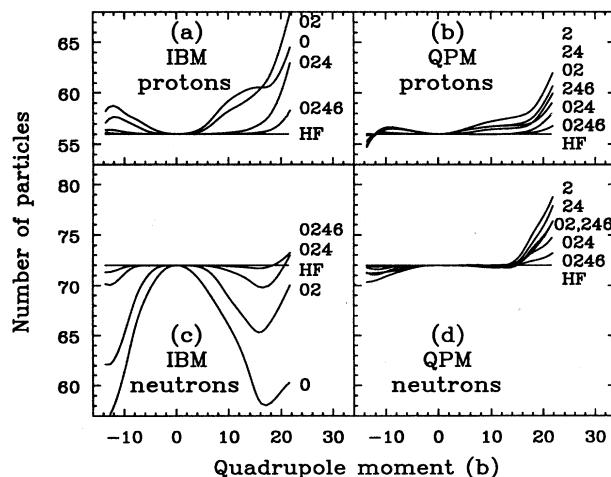


FIG. 7. Mean neutron and proton numbers of truncated states, for the IBM, (a) and (c), and the QPM, (b) and (d), reference state, compared with the values for ^{128}Ba .

the discrepancies in particle numbers induce differences in energy of many tens of MeV, far beyond the energy range of the deformation effects, which we want to analyze. Some insight in the quality of description of the HF energy by the truncated pairs can, however, be gained by comparing the corresponding scaled energies per particle, $128 \times E / \langle A \rangle$, where E is the HF energy, Eq. (2.4), calculated for the truncated state, Eq. (4.2), $\langle A \rangle$ stands for the mean number of nucleons in the same truncated state, and 128 is the scale factor corresponding to the correct number of nucleons in ^{128}Ba .

The scaled HF energies per particle of the truncated states are shown in Figs. 8(a) and 8(b) for the IBM and QPM cores, respectively, and compared with the untruncated values. For both cores, one obtains a poor agreement with the self-consistent energies, and almost no deformation can be created, when only the dominant components are kept. The energy for the $J=2$ pair of the QPM is similar to the energy for the 02 pairs of the IBM. The former is lower than the latter for large deformations and higher for small deformations. For the IBM core, the prolate and oblate equilibrium deformations can be reproduced only when the 0246 components are included, and even the inclusion of all 0...10 components is not able to reproduce the HF energy at the far end of prolate deformations. For the QPM core, the equilibrium deformations are reproduced by the 024 components. The energies for the truncations to 24 and 246 cluster between those for 02 and 2, and are not plotted in Fig. 8(b). Without the $J=0$ component of the QPM pair, one cannot reproduce the equilibrium deformation at all. However, when this component is included, the energy for a

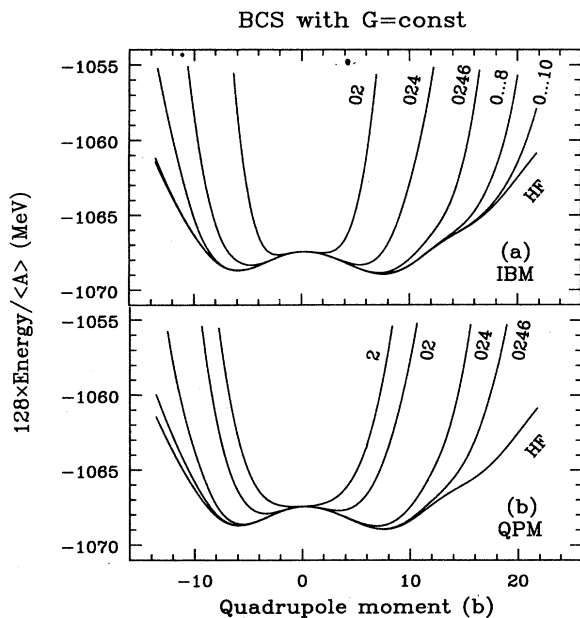


FIG. 8. Scaled energy per particle of the truncated states, for the IBM (a) and the QPM (b) reference state, compared with the HF results. The $G = \text{const}$ version of the BCS approach has been used.

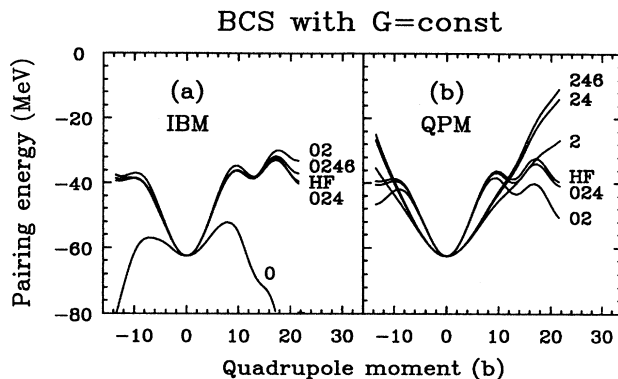


FIG. 9. Pairing energy of the truncated states, for the IBM (a) and the QPM (b) reference state, compared with the HF results. The $G = \text{const}$ version of the BCS approach has been used.

given truncation of the QPM pair is always lower than for the same truncation of the IBM pair. This suggests that the QPM reference state is better suited for a description of deformed states in terms of low- J quasiparticle pairs than the IBM reference state.

A role played by the $J=0$ pairs can be seen from Fig. 9, where we plot the pairing energy, Eq. (2.5), for different truncations of the IBM (a) and the QPM (b) pairs. One can see that the S pair of the IBM cannot alone account correctly for the pairing correlations with increasing deformation. However, when the D pair is added, the HF pairing energy is reproduced very well.

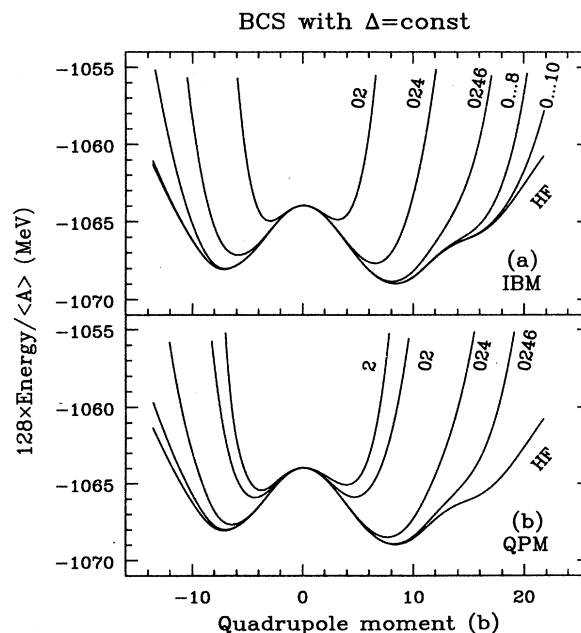


FIG. 10. Scaled energy per particle of the truncated states, for the IBM (a) and the QPM (b) reference state, compared with the HF results. The $\Delta = \text{const}$ version of the BCS approach has been used.

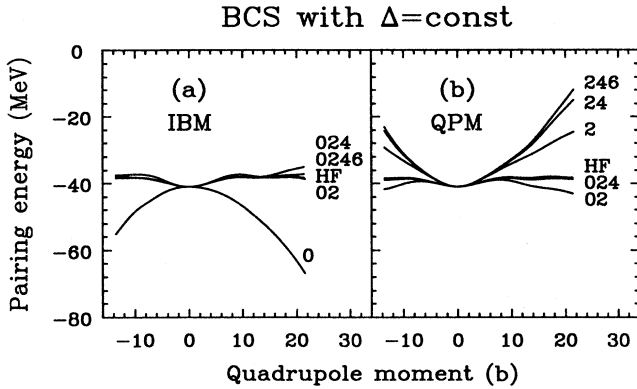


FIG. 11. Pairing energy of the truncated states, for the IBM (a) and the QPM (b) reference state, compared with the HF results. The $\Delta=\text{const}$ version of the BCS approach has been used.

Since both pairs are of the same order, $x_0^2 \simeq x_2^2$, one can say that both are equally important for the pairing effects. The pairing energy is equally well described by the QPM pairs, provided that at least $J=0$ and 2 pairs are included. Without the $J=0$ pair, the pairing energy has qualitatively different behavior than the untruncated one. The sudden decrease of the absolute value of the HF pairing energy, which occurs for small deformations and is related to a sudden change in level density (Sec. II), cannot be obtained unless the \mathcal{S} pair is included. From these results it is clear that the original assumption of the QPM, in which solely the \mathcal{D} pair has been introduced, has to be modified by adding the \mathcal{S} pair, which is necessary when the pairing and quadrupole effects are interwoven.

In Fig. 10 we show for comparison the scaled energies for truncated states obtained from the calculation with constant pairing gaps ($\Delta=\text{const}$ version). It can be seen that, although the HF energies are quite different in the $G=\text{const}$ and $\Delta=\text{const}$ versions, the quality of successive truncations is very much the same. The poor approximation of the HF curve with 2 and 02 components alone, and a relatively better result for the QPM core than for the IBM (at identical truncations), are evident. Inclusion of the $J=4$ ($J=6$) component is necessary to reproduce the equilibrium deformation for the QPM (IBM) core. Still higher- J pairs must be included if the HF curve is to be reproduced up to the largest studied deformations. Despite the fact that the pairing energies in the $\Delta=\text{const}$ version, Fig. 11, are different from those in the $G=\text{const}$ version, the conclusions which one can draw about the role of the $J=0$ pairs are the same.

C. Core and vacuum polarization

The interacting boson model assumes that the quadrupole collective states are built of S and D pairs of *valence particles* (or *valence holes* past midshell). From this assumption, it can be derived that the number of active pairs is equal to half of the number of valence particles (or holes). Since the IBM pairs \hat{Z}^\dagger , which transform the IBM reference state $|\Psi_{\text{ref}}\rangle$ (^{132}Sn nucleus, see Sec. III)

into the deformed state of ^{128}Ba through creation of some number of quasiparticles, Eqs. (3.6) and (3.7), are *a priori* built of all single-particle states, we are able to verify the above assumption of the IBM. In Fig. 12 we present the mean neutron and proton quasiparticle numbers, N^{qp} and Z^{qp} , respectively, defined as

$$N^{qp} = \langle \Psi | \sum_{\mu,n} \alpha_{\mu,n}^\dagger \alpha_{\mu,n} | \Psi \rangle, \quad Z^{qp} = \langle \Psi | \sum_{\mu,p} \alpha_{\mu,p}^\dagger \alpha_{\mu,p} | \Psi \rangle. \quad (4.5)$$

where $\alpha_{\mu,n}^\dagger$ and $\alpha_{\mu,n}$ are the quasiparticle operators corresponding to the IBM reference state $|\Psi_{\text{ref}}\rangle$. Had the IBM neutron (proton) quasiparticle pairs been equal to the *valence neutron hole (proton particle)* pairs added to ^{132}Sn , the mean neutron (proton) quasiparticle number would have been for all deformations equal to 10 (6), which is the difference of number of neutrons (protons) in ^{132}Sn and ^{128}Ba . As seen in Fig. 12, this is obviously not the case, the quasiparticle numbers increase substantially with deformation. At the spherical shape, the neutron and proton quasiparticle numbers are approximately equal to 11 and 7, respectively. (The difference of about one quasiparticle illustrates the fact that the spherical self-consistent single-particle states in ^{132}Sn and ^{128}Ba are not identical.) These numbers are much larger for large prolate and oblate deformations. The increase of quasiparticle numbers is even bigger for the truncated states than for the HF states.

The quasiparticle numbers with respect to the QPM core $|\Psi'_{\text{ref}}\rangle$ are also given in Fig. 12. By definition they are equal to zero at the spherical shape. With increasing deformation these numbers increase, which is entirely consistent with assumptions of the QPM, where the deformation is generated by adding quasiparticle pairs to the spherical core. One should note that in the QPM the truncation affects the quasiparticle numbers much less than it does in the IBM.

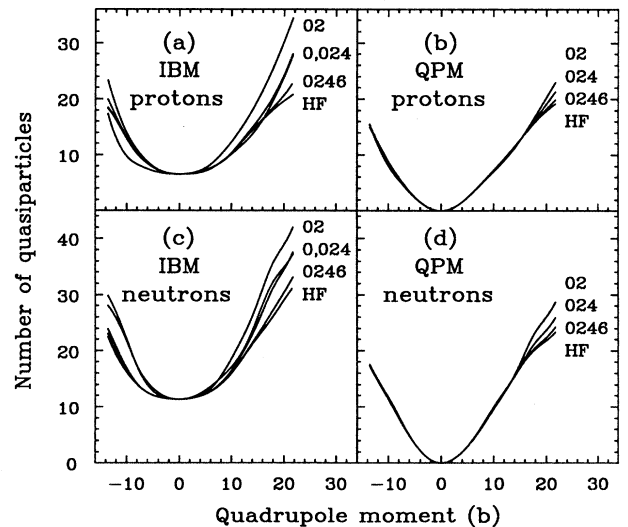


FIG. 12. Mean number of neutron and proton quasiparticles in the truncated states, for the IBM, (a) and (c), and the QPM, (b) and (d), reference state, compared with the HF results.

As seen from the above results, the quasiparticle HF pairs are not confined to the valence space. In order to estimate quantitatively the role of different single-particle states in building up the nuclear deformation, let us split the set of the single-particle states of the reference state into three following classes according to their single-particle energies. For ^{128}Ba the major valence shell consists of states between the magic numbers 50 and 82, both for neutrons and for protons. Therefore, we will call the 50 lowest single-particle states the hole states, next 32 the valence states and all the other the particle states. The single-particle index μ will be denoted by h , v , or p depending on which value it assumes. One should note that this definition explicitly refers to the single-particle energies of the reference state, and in what follows, when discussing the properties of the IBM (QPM) pairs, we define the hole, valence, and particle states with respect to the IBM (QPM) reference state. By core and vacuum polarization effects we will understand the influence of the hole and particle states, respectively, on the properties of deformed states and of the quasiparticle pairs. Holes and particles are now considered as states below and above, respectively, the valence space, and not below and above the Fermi level, as is usual.

The quasiparticle numbers, Eq. (4.5), can now be presented as sums of contributions coming from the hole, valence, and particle space, which for neutron states read

$$\begin{aligned} N^{qp} &= N_H^{qp} + N_V^{qp} + N_P^{qp}, \\ N_H^{qp} &= \left\langle \Psi \left| \sum_{h,n} \alpha_h^\dagger \alpha_h \right| \Psi \right\rangle, \\ N_V^{qp} &= \left\langle \Psi \left| \sum_{v,n} \alpha_v^\dagger \alpha_v \right| \Psi \right\rangle, \\ N_P^{qp} &= \left\langle \Psi \left| \sum_{p,n} \alpha_p^\dagger \alpha_p \right| \Psi \right\rangle, \end{aligned} \quad (4.7)$$

and similarly for protons. The HF quasiparticle numbers are presented in Fig. 13 together with their constituents

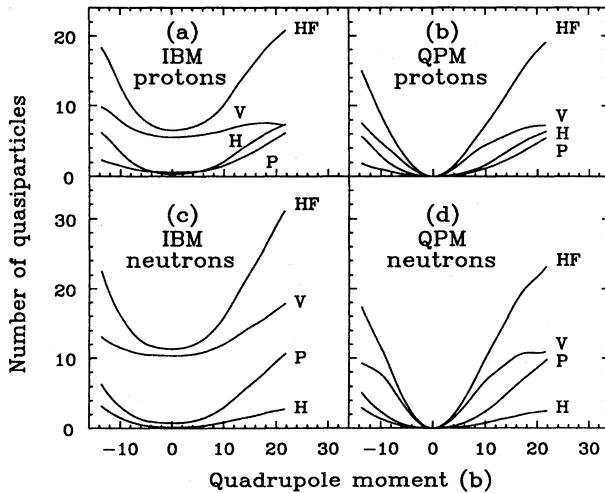


FIG. 13. Mean number of neutron and proton quasiparticles in the valence (V), hole (H), and particle (P) space, Eq. (4.7), for the IBM, (a) and (c), and the QPM, (b) and (d), reference state.

given by Eq. (4.7). It is seen that for the IBM core, Fig. 13(a) and (c), the increase of the neutron quasiparticle number with deformation is mainly caused by the increase of number of quasiparticles in the valence and in the particle space, while the proton quasiparticle number increases due to the components in the hole and in the particle space. On the average, the effects of the hole and particle spaces are comparable with effects inherent to the valence space, i.e., the core and vacuum polarization plays a substantial role in building up the nuclear deformation. In accordance with the position of the Fermi level in the valence shell, which for neutrons (protons) is closer to the upper (lower) limit of this space, the vacuum polarization is more important for neutrons, while the core polarization is more important for protons. Similar conclusions are valid for the QPM quasiparticle numbers, Figs. 13(b) and (d).

In order to directly estimate the fractions of the quasiparticle pairs which are located outside the valence space we define the valence-valence (VV) and valence-hole (VH) pair amplitudes by

$$\begin{aligned} y_J^{VV} &= \sum_{vv'} |Z_{Jvv'}|^2, \\ y_J^{VH} &= 2 \sum_{vh} |Z_{Jvh}|^2, \end{aligned} \quad (4.8)$$

where the factor 2 in the definition of y_J^{VH} accounts for the antisymmetry of the Z_J matrix. Analogously, one can define all the other components: PP, HH, PV, and PH. Because of the normalization defined in Eq. (3.16),

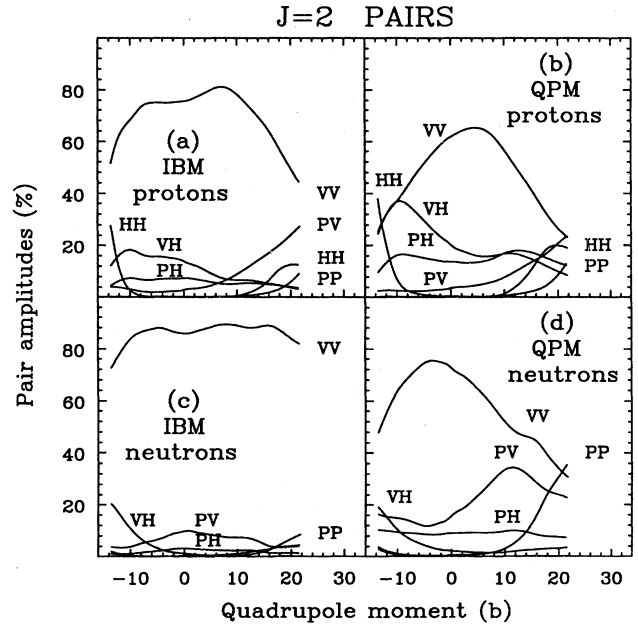


FIG. 14. Pair amplitudes of the $J=2$ quasiparticle pairs, for the IBM, (a) and (c), and the QPM, (b) and (d), reference state. The valence-valence (VV) and valence-hole (VH) amplitudes are calculated according to Eq. (4.8). Analogous formulae are used to determine the remaining four amplitudes, PP, PV, PH, and HH.

the sum of the six y_j pair amplitudes is equal to 1,

$$y_j^{\text{HH}} + y_j^{\text{YV}} + y_j^{\text{PP}} + y_j^{\text{YH}} + y_j^{\text{PH}} + y_j^{\text{PV}} = 1, \quad (4.9)$$

and the importance of a given component is quantitatively described by the corresponding y_j amplitude.

We have calculated such pair amplitudes for the dominant components of HF pairs for both considered cores. It turns out that the IBM $J=0$ neutron pair is well concentrated in the valence-valence space; the corresponding y_j^{YV} amplitude is for all deformations larger than 90%. The same amplitude for the IBM $J=0$ proton pair is larger than 90% between $Q = -10b$ and $10b$, and then drops significantly to 55% (70%) on the prolate (oblate) side. The amplitudes for the neutron and proton $J=2$ pairs are presented in Fig. 14. It can be seen that the neutron (proton) valence-valence (VV) component amounts in the deformation range between $Q = -8b$ and $10b$ to 90% (80%) of the IBM $J=2$ pair, Figs. 14(a) and (c). For protons the VV component decreases rapidly with increasing deformation outside the above mentioned range, and the other components start to increase (especially PV and HH on the prolate and oblate side, respectively). For the QPM core, Figs. 14(b) and (d), the highest percentage of the VV component is smaller, 80% and 65% for neutrons and protons, respectively, and this component decreases rather rapidly with increasing deformation, reaching 50% around the equilibrium deformation.

V. VARIATION AFTER TRUNCATION

The variation after truncation consists in freely adjusting the low angular-momentum pairs, so as to minimize the HF energy for a given quadrupole moment and correct mean particle numbers. In order to find such optimal pairs, we have used the gradient method. The HF energy can be considered either as a function of the quasiparticle pair matrix Z , or of the particle pair matrix C , see Sec. III. The gradient of the energy with respect to the C matrix, $(\nabla_C E)_{\mu\nu} = \partial E / \partial C_{\mu\nu}$, reads

$$-\nabla_C E = (1-\rho)h\kappa + \kappa h^*(1-\rho^*) + \kappa\Delta^*\kappa + (1-\rho)\Delta(1-\rho^*), \quad (5.1)$$

where h and Δ are the matrices of the mean field and of the pairing field, respectively, and ρ and κ are the density matrix and the pairing tensor (definitions from Ref. 27 are used). In the BCS approximation, which we use here, the only nonvanishing elements of the Δ matrix are the ones between the time-reversed states, i.e.,

$$\Delta_{\mu\nu} = s_\mu \Delta \delta_{\bar{\mu}\nu}, \quad (5.2)$$

where Δ is the constant gap parameter [in the $\Delta = \text{const}$ version, Eq. (2.1)] or is determined from the pairing strength G [in the $G = \text{const}$ version, Eq. (2.6)]. Since the quasiparticle pair \hat{Z}^\dagger is given in terms of the quasiparticle creation operators α_μ^\dagger , Eq. (3.7), and the particle pair \hat{C}^\dagger in terms of the particle operators a_μ^\dagger , Eq. (3.3), the quasiparticle gradient $\nabla_Z E$ can be expressed through the particle gradient $\nabla_C E$ as

$$\nabla_Z E = A_{\text{ref}}^\dagger (1 + C_{\text{ref}}^\dagger C) (\nabla_C E) (1 + C C_{\text{ref}}^\dagger) A_{\text{ref}}^*, \quad (5.3)$$

where A_{ref} and C_{ref} correspond to the Bogolyubov transformation $|0\rangle \rightarrow |\Psi_{\text{ref}}\rangle$, see Fig. 3 and Eq. (3.9).

The condition for the absolute minimum of energy at given mean particle numbers reads

$$\nabla_Z E - \lambda_n \nabla_Z N_n - \lambda_p \nabla_Z N_p = 0, \quad (5.4)$$

where N_n and N_p are mean neutron and proton numbers as functions of the Z matrix, and λ_n and λ_p are the corresponding Lagrange multipliers. The quasiparticle gradients of particle numbers, $\nabla_Z N_n$ and $\nabla_Z N_p$ can be calculated from the corresponding particle gradients given by

$$\begin{aligned} \nabla_C N_n &= (1-\rho_n)\kappa_n + \kappa_n(1-\rho_n^*), \\ \nabla_C N_p &= (1-\rho_p)\kappa_p + \kappa_p(1-\rho_p^*), \end{aligned} \quad (5.5)$$

in analogy to Eq. (5.3). It is easy to check that condition (5.4), which is equivalent to the similar condition for the particle gradients, leads to the well known BCS expressions for the occupation probabilities.

In order to find the minimum of energy with respect to the quasiparticle matrix \tilde{Z} truncated to some angular momenta, one has to solve the Eq. (5.4) truncated to the same angular momenta, i.e.,

$$\nabla_{\tilde{Z}} E - \lambda_n \nabla_{\tilde{Z}} N_n - \lambda_p \nabla_{\tilde{Z}} N_p = 0, \quad (5.6)$$

where, as in Sec. IV, tilde denotes truncation of some angular momentum components. A practical method of approaching the minimum (the projected gradient method²⁷) consists in correcting the truncated matrix \tilde{Z} , Eq. (4.1), by subtracting the truncated gradient [left-hand side of Eq. (5.6)] multiplied by a suitable small coefficient ϵ , i.e.,

$$\tilde{Z} \rightarrow \tilde{Z} - \epsilon (\nabla_{\tilde{Z}} E - \lambda_n \nabla_{\tilde{Z}} N_n - \lambda_p \nabla_{\tilde{Z}} N_p). \quad (5.7)$$

The value $\epsilon = 3 \text{ keV}^{-1}$ has been used in our calculations. The Lagrange multipliers λ_n and λ_p have now to be iteratively corrected to guarantee the desired number of neutrons and protons for a solution of Eq. (5.6).

Unfortunately, the projected gradient method is numerically much more time consuming, roughly by an order of magnitude, than the usual methods used to solve the HF equations. The standard methods cannot be applied because Eq. (5.6) is not equivalent to a requirement that the self-consistent mean field h is diagonal in the basis diagonalizing ρ , as is the case for Eq. (5.4).

The gradients of energy with respect to two matrices Z and Z' , corresponding to two different reference states, are related by

$$\nabla_{Z'} E = \mathcal{U}_0^\dagger (1 + Z_0^\dagger Z) \nabla_Z E (1 + Z Z_0^\dagger) \mathcal{U}_0^*, \quad (5.8)$$

[see Eq. (3.17) and (3.20)]. Again it is seen, that as soon as the Z matrix differs from a scalar one, the truncated gradient $\nabla_{\tilde{Z}} E$ and the truncated gradient $\nabla_{\tilde{Z}'} E$ are not identical, and therefore the corresponding variational equations give different solutions.

The energies resulting from our variation after trunca-

tion calculations for ^{128}Ba are presented in Fig. 15. The calculations have been performed for truncations to the angular momenta 02 and 024 (IBM), and to 2, 02, and 024 (QPM). In order to have substantial deformation energies for the HF solutions, we have used the $\Delta=\text{const}$ version of treatment of pairing correlations (see Sec. II). The truncation to dominant components, 02 for IBM and 2 for QPM, gives on the prolate side very similar energies for both cores. On the oblate side, the dominant pair of the QPM gives at moderate deformations the energy much lower than the dominant pairs of the IBM. In fact, it can even give the energy lower than the one for the truncation to 02. This apparently contradictory result is related to the fact that for the $\Delta=\text{const}$ version it is the quantity $E'=E+E_p$, Eq. (2.2), and not the energy E , which is minimized by the BCS theory. For a given truncation, the energies obtained for the QPM core are lower than those for the IBM core. The differences are, however, smaller than for the truncated HF pairs, cf., Fig. 10. This occurs because the decrease of energy due to the variation after truncation is larger for the IBM core than for the QPM core. In other words the truncated HF pairs are much closer to the optimal pairs for the QPM than for the IBM. This is especially visible for the truncation to 024 QPM pairs, where the variation after truncation gives almost the same energy as the truncated HF pairs. Still, however, the truncation to dominant components gives for both cores the deformation energy curve very different from the one of the HF method. Truncation to 024 allows for a fair description of the equilibrium deformation, while a large discrepancy still persists for larger deformations.

Pairing energy is plotted for various truncations in Fig. 16. Again one can see that for a given truncation the pairing energies are closer to the HF values for the QPM core than for the IBM core. The pairing energy for the dominant (2) pair of the QPM depends on the deformation in a qualitatively different way than those for truncation with the $J=0$ pair included. This confirms our previous conclusions, Sec. IV, about a crucial role of the $J=0$ component in describing the pairing correlations.

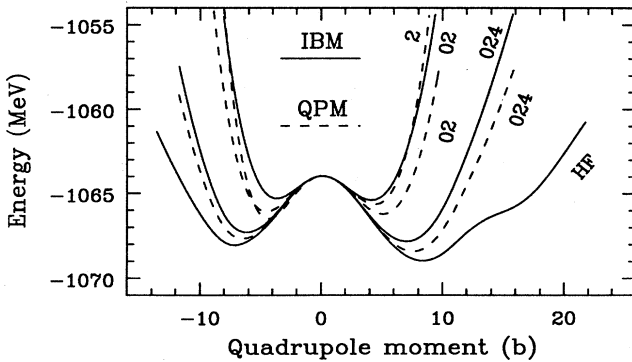


FIG. 15. Energy of truncated states obtained by the variation after truncation, for the IBM (solid lines) and the QPM (dashed lines) reference state, compared with the HF results.

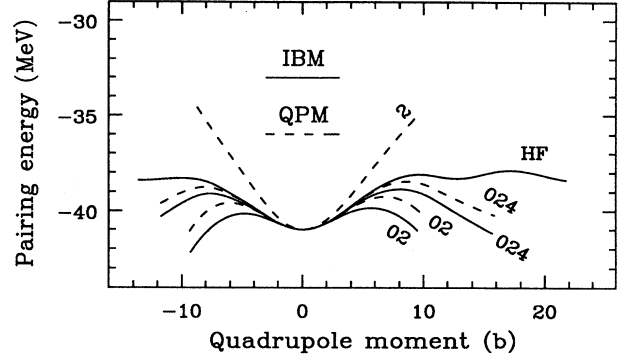


FIG. 16. Pairing energy for truncated states obtained by the variation after truncation, for the IBM (solid lines) and the QPM (dashed lines), compared with the HF results.

VI. TRUNCATION OF HF DENSITY MATRICES

The IBM and the QPM models assume that the basic building blocks of the quadrupole collective excitations are made of pairs of fermions coupled to angular momentum $J=2$. As opposed to this, the Bohr and Mottelson model¹⁻³ assumes that such excitations are related to fluctuations of the quadrupole component of the nuclear density. In this section we develop a method which allows us to present the HF energy of a deformed state as a multipole series associated with the multipole expansion of the density matrix. In this way we are able to discuss the quality of approximating this energy by the low- J terms, and to compare this approximation with energies of truncated states discussed in the previous sections.

Let the two-body interaction \hat{V} and the kinetic energy operator \hat{T} define the nuclear effective Hamiltonian \hat{H} :

$$\hat{H} = \hat{T} + \hat{V} = \sum_{\mu\nu} T_{\mu\nu} a_{\mu}^{\dagger} a_{\nu} + \frac{1}{4} \sum_{\mu\nu\kappa\lambda} V_{\mu\nu\kappa\lambda} a_{\mu}^{\dagger} a_{\nu}^{\dagger} a_{\lambda} a_{\kappa}. \quad (6.1)$$

Then the mean energy of a nuclear state $|\Psi\rangle$,

$$E = \text{Tr} T \rho + \frac{1}{4} \text{Tr} V \sigma = \sum_{\mu\nu} T_{\mu\nu} \rho_{\nu\mu} + \frac{1}{4} \sum_{\mu\nu\kappa\lambda} V_{\mu\nu\kappa\lambda} \sigma_{\kappa\lambda\mu\nu}, \quad (6.2)$$

is determined by the one- and two-body density matrices ρ and σ ,

$$\rho_{\nu\mu} = \langle \Psi | a_{\mu}^{\dagger} a_{\nu} | \Psi \rangle, \quad (6.3)$$

$$\sigma_{\kappa\lambda\mu\nu} = \langle \Psi | a_{\mu}^{\dagger} a_{\nu}^{\dagger} a_{\lambda} a_{\kappa} | \Psi \rangle. \quad (6.4)$$

The density matrices of deformed states are sums of various angular-momentum components and, for the symmetries imposed as in Sec. III, only even- J components contribute:

$$\rho = \rho_0 + \rho_2 + \rho_4 + \dots, \quad (6.5)$$

$$\sigma = \sigma_0 + \sigma_2 + \sigma_4 + \dots, \quad (6.6)$$

in close analogy to the multipole expansion of the quasi-particle pair matrix, Eq. (3.15). Since the kinetic energy operator \hat{T} is a scalar operator, and the same holds for

the true two-body interaction \hat{V} , the energy of the state $|\Psi\rangle$ depends *only* on the scalar parts ρ_0 and σ_0 of the density matrices,

$$E = \text{Tr}T\rho_0 + \frac{1}{4}\text{Tr}V\sigma_0. \quad (6.7)$$

When the state $|\Psi\rangle$ is a quasiparticle vacuum, the two-body density matrix σ is determined by the one-body density matrix ρ and the pairing tensor κ ,

$$\sigma_{\kappa\lambda\mu\nu} = \rho_{\kappa\mu}\rho_{\lambda\nu} - \rho_{\kappa\nu}\rho_{\lambda\mu} + \kappa_{\mu\nu}^*\kappa_{\kappa\lambda}. \quad (6.8)$$

The first term on the right-hand side is a product of one-body density matrices, typical for an uncorrelated many-particle system. The second term is the exchange term describing the Pauli correlations in a system of fermions, and the third term describes the pair correlations. The scalar component of σ , which determines the energy, Eq. (6.7), can be obtained by calculating the scalar parts of both sides of Eq. (6.8), i.e.,

$$\begin{aligned} \sigma_{0\kappa\lambda\mu\nu} = & \rho_{0\kappa\mu}\rho_{0\lambda\nu} - \rho_{0\kappa\nu}\rho_{0\lambda\mu} \\ & + \rho_{2\kappa\mu}\rho_{2\lambda\nu} - \rho_{2\kappa\nu}\rho_{2\lambda\mu} + \rho_{4\kappa\mu}\rho_{4\lambda\nu} - \rho_{4\kappa\nu}\rho_{4\lambda\mu} + \dots \\ & + \kappa_{0\mu\nu}^*\kappa_{0\kappa\lambda} + \kappa_{2\mu\nu}^*\kappa_{2\kappa\lambda} + \kappa_{4\mu\nu}^*\kappa_{4\kappa\lambda} + \dots, \end{aligned} \quad (6.9)$$

where the multipole expansion of the pairing tensor reads $\kappa = \kappa_0 + \kappa_2 + \kappa_4 + \dots$. The consecutive terms on the right-hand side of Eq. (6.9) describe an uncorrelated *spherically symmetric* system of fermions, its quadrupole-quadrupole, hexadecapole-hexadecapole, and higher correlations, and then the monopole, quadrupole, hexadecapole, and higher pair correlations. Inserting the expansion for σ_0 into Eq. (6.7) one obtains the series of terms

$$E = E_0 + E_2 + E_4 + \dots, \quad (6.10)$$

where E_0 is the monopole energy of the system,

$$E_0 = \text{Tr}T\rho_0 + \frac{1}{2}\text{Tr}\rho_0 V\rho_0 + E_P, \quad (6.11)$$

and E_2 and E_4 are the quadrupole and hexadecapole, respectively, correlation energies,

$$E_J = \frac{1}{2}\text{Tr}\rho_J V\rho_J = \frac{1}{2} \sum_{\mu\nu\kappa\lambda} \rho_{J\kappa\mu} V_{\mu\nu\kappa\lambda} \rho_{J\lambda\nu}, \quad J > 0. \quad (6.12)$$

Because in our study we use the monopole pairing interaction, the quadrupole, hexadecapole and higher pair correlations do not contribute to the pairing energy, which therefore is included in the monopole energy E_0 .

Now one should recall, that the Skyrme interaction depends on the nuclear density, and hence for a deformed system is not rotationally invariant. In such a case, when trying to separate the total energy of the deformed system into multipole correlation energies, one can express the energy by the self-consistent potential Γ ,

$$E = \text{Tr}T\rho + \frac{1}{2}\text{Tr}\Gamma\rho + E_P, \quad (6.13)$$

$$\Gamma_{\mu\kappa} = \sum_{\nu\lambda} V_{\mu\nu\kappa\lambda} \rho_{\lambda\nu}, \quad (6.14)$$

and then use the multipole expansion of the density matrix, Eq. (6.5). As a result one obtains the series of Eq. (6.10) with the monopole energy E_0 and the multipole

correlation energies E_J , $J > 0$, given by

$$E_0 = \text{Tr}T\rho_0 + \frac{1}{2}\text{Tr}\Gamma\rho_0 + E_P, \quad (6.15)$$

$$E_J = \frac{1}{2}\text{Tr}\Gamma\rho_J, \quad J > 0. \quad (6.16)$$

Since the trace is a scalar operation, one has

$$\text{Tr}\Gamma\rho_J = \text{Tr}\Gamma_J\rho_J, \quad (6.17)$$

where Γ_J is the rank J multipole component of the self-consistent potential Γ , and the multipole correlation energies describe the correlations between the multipole components of the mean field and of the density matrix. These correlation energies take explicitly into account the rearrangement effects resulting from the density dependence of the effective interaction. For scalar interactions they reduce to previously derived formula, Eq. (6.12), because then the rank J component of the self-consistent potential depends only on the rank J component of the density matrix.

In Fig. 17 we show the series of correlation energies, Eq. (6.10), truncated to low angular momenta, $0 \leq J \leq J_{\max}$, for $J_{\max} = 0, \dots, 6$, denoted as 0, 02, 024, and 0246. The truncated energies converge to the HF energy, and this convergence is much faster than the one corresponding to truncations of multipole components of coherent quasiparticle pairs, cf., Fig. 8. The inclusion of the 0246 components gives energies which in the scale of the figure cannot be distinguished from the HF results, and even the 024 components assure quite good agreement. The 02 components are good enough to fairly well describe the equilibrium deformation, and give similar energies as the 024 components of the QPM quasiparticle pair. These results show that the low- J multipole components of the density matrix better account for the energy of the deformed state than the low- J multipole components of the IBM or QPM quasiparticle pairs, i.e., the microscopic concept underlying the description of quadrupole collective motion within the Bohr and Mottelson model is better compatible with the HF results than the assumptions of the IBM or QPM.

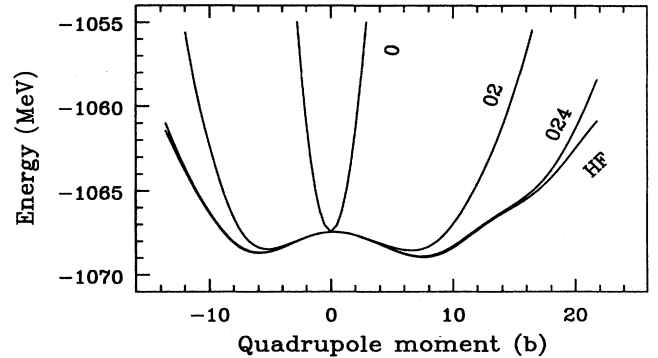


FIG. 17. Monopole energy $E_0(0)$, and the sums $E_0 + E_2$ (02) and $E_0 + E_2 + E_4$ (024) which take into account the quadrupole and the hexadecapole correlation energies, E_2 and E_4 , compared with the HF energy.

A disadvantage of the truncation of density matrix, with respect to the truncation of quasiparticle pairs consists in the fact that the truncated density matrix *does not*, in general, correspond to any nuclear state. This can be seen by considering the relation between the one-body density matrix and the pairing tensor,

$$\rho = \rho^2 + \kappa\kappa^\dagger, \quad (6.18)$$

which is valid for any quasiparticle vacuum. Since $\kappa\kappa^\dagger$ is a positive definite matrix, the eigenvalues of ρ are located between 0 and 1. Such condition for the eigenvalues of the density matrix stems directly from the Pauli exclusion principle, and must be satisfied for any ρ which is a one-body density matrix of a many fermion system. Calculating the scalar components of both sides of Eq. (6.18), one obtains

$$\rho_0 = \rho_0^2 + \rho_2^2 + \rho_4^2 + \dots + \kappa_0\kappa_0^\dagger + \kappa_2\kappa_2^\dagger + \kappa_4\kappa_4^\dagger + \dots, \quad (6.19)$$

which guarantees that the eigenvalues of ρ_0 are between 0 and 1, and proves that the scalar component of the density matrix is a one-body density matrix with correctly incorporated Pauli exclusion. On the other hand, truncating Eq. (6.18) to some angular momenta $0 \leq J \leq J_{\max}$ for $J_{\max} > 0$, one cannot conclude the same about the truncated density matrix $\rho_0 + \dots + \rho_{J_{\max}}$.

In order to illustrate the effect of truncation on the eigenvalues of the density matrix, we plotted, in Fig. 18, the maximal and minimal eigenvalues of the truncated density matrix $\rho_0 + \dots + \rho_{J_{\max}}$ as functions of the HF quadrupole moment. Outside a small region of deformations around the spherical point, the eigenvalues of $\rho_0 + \dots + \rho_{J_{\max}}$ escape the allowed interval between 0 and 1. The maximal eigenvalues increase above 1 and the minimal ones become negative, the magnitude of these changes being of the order of 0.1. Even for $J_{\max} = 10$, when no significant trace of the truncation can be seen in the energy, the violation of Pauli principle by the truncated density matrix is still visible.

VII. CONCLUSIONS

We have analyzed from the microscopic point of view the assumptions made by three collective models of quadrupole motion: The unified Bohr and Mottelson (BM) model, the interacting boson model (IBM), and the quadrupole phonon model (QPM). The analysis has been performed by checking the ability of these models to reproduce the properties of deformed states of ^{128}Ba obtained within the Hartree-Fock theory with the Skyrme interaction. The following conclusions can be drawn from our study. (i) The dominant angular-momentum components of fermion pairs, S and D for the IBM and \mathcal{D} for the QPM, are not sufficient to describe the equilibrium defor-

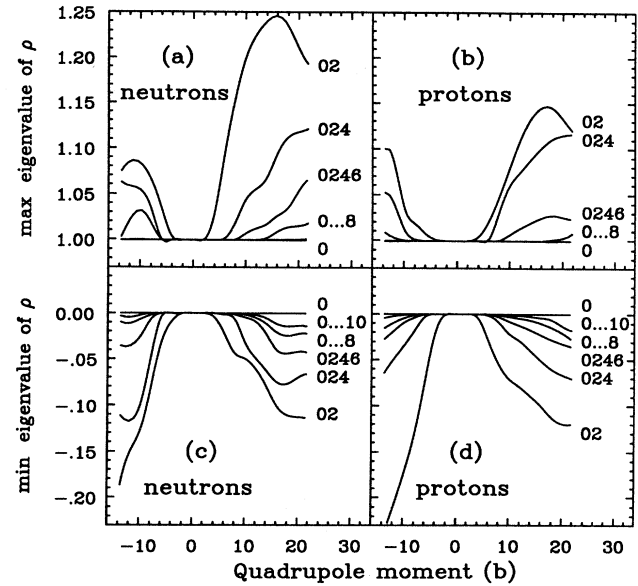


FIG. 18. Maximal, (a) and (b), and minimal, (c) and (d), eigenvalues of the truncated neutron and proton density matrix.

mation of ^{128}Ba . This is especially manifest from our results obtained by the variation after truncation, which give the lower bounds for the energy of condensates of such fermion pairs. (ii) Inclusion of $J=0, 2$, and 4 components (both in the IBM and QPM) allows to fairly well describe the equilibrium properties of the studied nucleus. The $J=0(\mathcal{S})$ pair of the QPM can be associated with a description of the pairing correlations. (iii) For a given truncation of the angular-momentum components, the QPM pairs better describe the deformed states than the IBM pairs. The truncated HF pairs of the QPM are closer to the optimal pairs, obtained by the variation after truncation, than those of the IBM. (iv) Core and vacuum polarization effects are fairly strong. A substantial, and increasing with deformation, part of the IBM pair is located outside the valence space. The number of active IBM pairs depends on deformation, and is equal to the values proposed by the IBM only in the vicinity of the spherical shape. (v) The HF equilibrium deformation is fairly well described by including only the quadrupole correlation energy, as suggested by the BM model. The quality of the description is comparable to the one obtained when the $J=0, 2$, and 4 components are included in the IBM and QPM pairs.

This work was supported in part by the Polish Ministry of National Education under Contract No. CPBP 01.09.

*Permanent address: Institute of Theoretical Physics, Warsaw University, Hoża 69, PL-00-681 Warsaw, Poland.

¹A. Bohr, Mat. Fys. Medd. Dan. Vid. Selsk. **26**, No. 14 (1952).

²A. Bohr and B. R. Mottelson, Mat. Fys. Medd. Dan. Vid. Selsk. **27**, No. 16 (1953).

³A. Bohr and B. R. Mottelson, *Nuclear Structure* (Benjamin, New York, 1975), Vol. 2.

⁴A. Arima and F. Iachello, Phys. Rev. Lett. **35**, 1069 (1975); Ann. Phys. (N.Y.) **99**, 253 (1976); **111**, 201 (1978); **123**, 468 (1979).

- ⁵D. Janssen, R. V. Jolos, and F. Dönau, Nucl. Phys. **A224**, 93 (1974).
- ⁶T. Otsuka, A. Arima, and F. Iachello, Nucl. Phys. **A309**, 1 (1978).
- ⁷A. Bohr and B. R. Mottelson, Phys. Scr. **22**, 468 (1980).
- ⁸J. Dukelsky, G. G. Dussel, and H. M. Sofia, Phys. Lett. **100B**, 367 (1981); Nucl. Phys. **A373**, 267 (1982).
- ⁹T. Otsuka, A. Arima, and N. Yoshinaga, Phys. Rev. Lett. **48**, 387 (1982).
- ¹⁰D. R. Bes, R. A. Broglia, E. Maglione, and A. Vitturi, Phys. Rev. Lett. **48**, 1001 (1982).
- ¹¹S. Pittel and J. Dukelsky, Phys. Lett. **128B**, 9 (1983).
- ¹²N. Yoshinaga, A. Arima, and T. Otsuka, Phys. Lett. **143B**, 5 (1984).
- ¹³W. Pannert, P. Ring, and Y. K. Gambhir, Nucl. Phys. **A443**, 189 (1985).
- ¹⁴J. Dukelsky, S. Pittel, H. M. Sofia, and C. Lima, Nucl. Phys. **A456**, 75 (1986); J. Dukelsky, G. G. Dussel, and H. M. Sofia, J. Phys. G **11**, L91 (1985).
- ¹⁵J. Dukelsky and S. Pittel, Phys. Lett. **B 177**, 125 (1986).
- ¹⁶C. H. Druce and S. A. Moszkowski, Phys. Rev. C **33**, 330 (1986).
- ¹⁷L. C. De Winter, N. R. Walet, P. J. Brussard, K. Allart, and A. E. L. Dieperink, Phys. Lett. **B 179**, 322 (1986).
- ¹⁸L. C. De Winter, N. R. Walet, and P. J. Brussard, Nucl. Phys. **A486**, 235 (1988).
- ¹⁹F. Iachello and I. Talmi, Rev. Mod. Phys. **59**, 339 (1987).
- ²⁰J. Dobaczewski and J. Skalski, Phys. Rev. C **38**, 580 (1988).
- ²¹A. Coc, P. Bonche, H. Flocard, and P. H. Heenen, Phys. Lett. **B 192**, 263 (1987).
- ²²D. Vautherin, Phys. Rev. C **7**, 296 (1973).
- ²³H. Flocard, P. Quentin, A. K. Kerman, and D. Vautherin, Nucl. Phys. **A203**, 433 (1973).
- ²⁴M. Beiner, H. Flocard, N. Van Giai, and P. Quentin, Nucl. Phys. **A238**, 29 (1975).
- ²⁵A. H. Wapstra and G. Audi, Nucl. Phys. **A432**, 1 (1985).
- ²⁶Assuming the generalized seniority scheme, one can prove the equivalence of the IBM and QPM, see A. B. Johnson and C. M. Vincent, Phys. Rev. C **25**, 1595 (1982). Although this assumption is not rigorously fulfilled for the deformed states, the reduction of the scalar component in the QPM, which we derive from Eq. (3.21), has the same origin.
- ²⁷P. Ring and P. Schuck, *The Nuclear Many-Body Problem* (Springer, New York, 1980).